Hypoxia promotes erythroid differentiation through the development of progenitors and proerythroblasts

Aditi Bapat[a], **Natascha Schippel**[a], **Xiaojian Shi**[b], **Paniz Jasbi**[b], **Haiwei Gu**[b], **Mrinalini Kala**[c], **Aparna Sertil**[a], **Shalini Sharma**[a]

[a]Department of Basic Medical Sciences, College of Medicine-Phoenix, University of Arizona, Phoenix, AZ

[b]Arizona Metabolomics Laboratory, College of Health Solutions, Arizona State University, Scottsdale, AZ

[c]Flow Cytometry Core, College of Medicine–Phoenix, University of Arizona, Phoenix, AZ

Abstract

Oxygen is a critical noncellular component of the bone marrow microenvironment that plays an important role in the development of hematopoietic cell lineages. In this study, we investigated the impact of low oxygen (hypoxia) on ex vivo myeloerythroid differentiation of human cord blood-derived CD34$^+$ hematopoietic stem and progenitor cells. We characterized the culture conditions to demonstrate that low oxygen inhibits cell proliferation and causes a metabolic shift in the stem and progenitor populations. We found that hypoxia promotes erythroid differentiation by supporting the development of progenitor populations. Hypoxia also increases the megakaryoerythroid potential of the common myeloid progenitors and the erythroid potential of megakaryoerythroid progenitors and significantly accelerates maturation of erythroid cells. Specifically, we determined that hypoxia promotes the loss of CD71 and the appearance of the erythroid markers CD235a and CD239. Further, evaluation of erythroid populations revealed a hypoxia-induced increase in proerythroblasts and in enucleation of CD235a$^+$ cells. These results reveal the extensive role of hypoxia at multiple steps during erythroid development. Overall, our work establishes a valuable model for further investigations into the relationship between erythroid progenitors and/or erythroblast populations and their hypoxic microenvironment.

The bone marrow microenvironment plays a vital role in normal hematopoiesis and in the pathophysiology of hematological malignancies [1–3]. A variety of cell types, including sinusoidal endothelial cells, mesenchymal stem cells, osteoblasts, non-myelinating Schwann cells, and mature hematopoietic cells such as macrophages and megakaryocytes, and noncellular components (e.g. cytokines) constitute the bone marrow microenvironment conducive for self-renewal of hematopoietic stem cells (HSCs) and their normal differentiation into the blood lineages [4–6]. Oxygen is a key noncellular component of this

microenvironment, where the gradient of oxygen varies from 1% in the areas adjacent to endosteal bone to 6% in the perivascular space [7]. Hematopoietic cells are distributed along this gradient, with stem cells located in the low-oxygen or hypoxic areas and proliferating progenitors and differentiating cells in the relatively oxygen-rich perivascular regions [8]. Exposure to hypoxic conditions has been reported to promote quiescence and maintenance of the undifferentiated stem phenotype of HSCs and improve their transplantation efficiency in immune-deficient mouse models [9–13]. In ex vivo assays, hypoxia has been reported to enhance formation of colony-forming units−granulocyte erythrocyte macrophage megakaryocyte (CFU-GEMM), burst-forming units−erythroid (BFU-E), and colony-forming unitserythroid (CFU-E), as well as the proliferation and differentiation of CFU-Es to erythroid precursors [14–16].

The hypoxic nature of the HSC niche is conducive for high rates of glycolysis and reduced tricarboxylic acid (TCA) cycle and oxidative phosphorylation activity [17–19]. These metabolic preferences provide long-term protection from oxidative stress related to reactive oxygen species. Onset of differentiation is accompanied by a shift in HSC metabolic phenotype, where demands on adenosine triphosphate (ATP) production are met by an increase in TCA cycle activity and oxidative phosphorylation. In addition to glucose, metabolism of amino acids and fatty acids also has been reported to be important for maintenance of HSC self-renewal and lineage commitment [9,20,21].

Myelo-erythroid differentiation of HSCs proceeds through a hierarchy of progenitors and lineage-committed cells that are characterized by well-defined surface markers [22,23]. Multipotent progenitors arising from HSCs give rise to the common myeloid progenitors (CMPs), which in turn form two lineage-restricted populations—megakaryoerythroid progenitor (MEP) or granulomonocytic progenitor (GMP). MEPs form megakaryocytes and erythrocytes, and GMPs form granulocytes and monocytes. Hypoxia has been found to drive this differentiation pathway toward the erythroid lineage as evidenced by formation of BFU-E and CFU-E colonies and enhanced expression of CD235a (glycophorin A) [14–16,24,25]. CFU-E cells form the proerythroblasts (ProE), which sequentially develop into basophilic erythroblasts (BasoE), polychromatic erythroblasts (PolyE), and orthochromatic erythroblasts (OrthoE) that undergo enucleation to become reticulocytes [26]. However, the effect of hypoxia on the distribution of progenitors in the CD34+ compartment and on erythroid maturation is not known. Additionally, studies have investigated but not found significant hypoxia-induced changes in the expression of other myeloid markers including CD33, CD41, CD11b, and CD14 [11,27].

In investigating the role of hypoxia during ex vivo myeloerythroid differentiation of human cord blood-derived CD34+ HSPCs, we found that low oxygen decreases proliferation of CD34+ cells and alters their metabolic properties. Hypoxia promotes erythroid differentiation by supporting the maintenance of progenitor populations and enhancing the formation of proerythroblasts and also significantly accelerates maturation of erythroid cells. Specifically, we found a hypoxia-associated increase in the loss of CD71 and in the appearance of the erythroid markers CD235a and CD239, as well as in enucleation of CD235a+ cells.

Methods

Isolation and culture of CD34+ cells

Umbilical cord blood (CB) units were obtained from Maricopa Integrated Health Services (MIHS now Valleywise Health, Arizona) through a material transfer agreement. CD34+ cells were isolated from the CB units as described previously [28,29]. Briefly, mononuclear cells (MNCs) were isolated using a Ficoll–Paque PLUS (GE Healthcare, Chicago, IL) gradient and stored frozen in liquid nitrogen. CD34+ cells were purified from MNCs using the magnetic activated cell sorting system (MACS) and the CD34+ microbead kit (Miltenyi Biotec, Bergisch Gladbach, Germany). Cells isolated from a single donor's CB were used for each experiment. MS-5 cells were maintained in Dulbecco's modified Eagle's medium (DMEM) with high glucose and L-glutamine (Thermo Fisher Scientific, Waltham, MA), 10% fetal bovine serum (FBS, Omega Scientific, Tarzana, CA) and 1% penicillin −streptomycin (Pen-Strep, Sigma-Aldrich, St. Louis, MO). For normoxic cultures, MS-5 cells were seeded at a density of 15,000/200 μL/well in a 48-well tissue culture coated plate 24 hours prior to CD34+ coculture (Supplementary Figure E1, online only, available at www.exphem.org). For hypoxia, cells were seeded at the same density 48 hours in advance. They were first incubated under normoxic conditions (21% O_2 and 5% CO_2) for 24 hours and then placed under hypoxic conditions (1% O_2 and 5% CO_2) in a ProOx hypoxia chamber (BioSpherix, Parish, NY) for 24 hours prior to coculture with CD34+ cells.

Freshly isolated CD34+ cells were incubated in 1 × stimulation medium (X-VIVO 15 serum-free medium containing 2 mM L-glutamine, 50 ng/mL stem cell factor (SCF), 50 ng/mL thrombopoietin (TPO), 20 ng/mL interleukin-3 (IL-3), and 50 ng/mL Flt3-Ligand) at a density of 1 × 10^5 cells per 200 μL in RetroNectin (20 ng/mL)-coated 48-well plates [23,28,29] (Supplementary Figure E1, online only, available at www.exphem.org). After 48 hours of stimulation, the cells were collected, washed in warm DMEM, and then layered on MS-5 cells in 1 × myeloid medium (MM) (DMEM with 10% FBS, 1% Pen-Strep, 50 ng/mL TPO, 5 ng/mL SCF, 4 units/mL erythropoietin [EPO], 5 ng/mL IL-3, and 5 ng/mL Flt3-Ligand) at densities of 5000/200 μL/well and 10,000/200 μL/well for normoxic and hypoxic cultures, respectively. Every 3–4 days, half of the myeloid medium was replaced with 2 × MM (DMEM containing 100 ng/mL TPO, 10 ng/mL SCF, 8 units/mL EPO, 10 ng/mL IL-3, and 10 ng/mL Flt3-Ligand). SCF, IL-3, and TPO were purchased from R&D Systems (Minneapolis, MN), and Flt3-Ligand and EPO were purchased from BioBasic (Amherst, NY).

Metabolite profiling

On day 4 after placing the CD34+ cells in normoxia and hypoxia, 200 μL of culture supernatant was collected from six different experiments (biological replicates) for metabolite profiling and stored frozen at −20°C. For MS-5 cultures, four replicates were collected. For metabolite extraction, the frozen samples were first thawed overnight at 4°C and prepared for MS as described [30]. A pooled sample, prepared by mixing all study samples, was used as the quality-control (QC) sample. All LC-MS/MS experiments were performed on an Agilent 1290 UPLC-6490 QQQ-MS system (Agilent Technologies, Santa Clara, CA) using a method developed over several studies [31–38], and has been described

previously [30]. The LC-MS system is equipped with an electrospray ionization (ESI) source and was controlled by Agilent Masshunter Workstation software. The extracted MRM peaks were integrated using Quantitative Data Analysis, and identity of metabolites was confirmed by comparison with known standards. Metabolites identified in supernatants of CD34$^+$ cell cocultures are listed in Supplementary Table E1 (online only, available at www.exphem.org), and those identified in supernatant of MS-5 cultures are listed in Supplementary Table E2 (online only, available at www.exphem.org). Fold change in metabolites in the spent medium was calculated relative to fresh medium ($1 \times$ MM) and log transformed prior to further analysis. Statistical comparisons to determine differences between hypoxia and normoxia used a significance threshold of $p < 0.05$. Principal component analysis and hierarchical clustering for heat map representation using fold change for all metabolites were performed in MetaboAnalyst.

Immunophenotyping and enucleation

For the stem and progenitor populations, cells from cultures in normoxia and hypoxia were collected, washed with FACS buffer ($1 \times$ phosphate-buffered saline [PBS] with 0.5% bovine serum albumin [BSA]), and then stained with antibodies to lineage markers (CD3, CD7, CD10, CD11b, CD19, and CD235a—all labeled with fluorescein isothiocyanate [FITC]), CD34 (APC-Cy7), CD38 (phycoerythrin [PE]), CD45RA (PE-Cy7), CD123 (APC), and CD133 (PE) in the dark for 20 min on ice. After incubation, cells were washed with FACS buffer, fixed with 1% paraformaldehyde (PFA) (Sigma Aldrich) for 10 min at room temperature, washed again, resuspended in FACS buffer, and then analyzed. 7-Aminoactinomycin D (7-AAD) was used as a viability dye to exclude dead cells. Unstained cells, single-stained controls, and fluorescence-minus-one (FMO) controls were used to set gates for positive populations using FlowJo software (TreeStar). Trypan blue viability counts were used to determine total numbers of live cells. The numbers of CD34$^+$ and CD133$^+$ HSCs were calculated using the percentages of CD34$^+$ and CD133$^+$ cells and the total cell number for each day of analysis. Fold change in the number of cells was calculated relative to day 1. For lineage populations, cells were stained with antibodies to CD34 (PerCP-Cy5.5), CD14 (APC-Cy7), CD66b (PE-Cy7), CD41a (PE), and CD235a (APC) and analyzed as described above. For analysis of the erythroid populations, cells were stained with antibodies to human CD34 (PerCP-Cy5.5), CD71 (PE-Cy7), CD105 (FITC), CD235a (APC), and CD239 (PE) and analyzed as described above. The CD34$^-$/Live population was used to calculate the percentage of positive cells. For analysis of the erythroblast populations, cells were stained with antibodies to human CD34 (APC-Cy7), CD235a (PE-Cy7), CD49d (APC), and CD233 (FITC).

For enucleation analysis, cells were stained with antibodies to CD34 (APC-Cy7) and CD235a (APC) and washed as described above, and then incubated with 100 nmol/L SYTO16 (excitation/emission 488/518 nm, Thermo Fisher Scientific), a live cell permeant dye, for 15 min at room temperature [39]. Nucleated and enucleated erythroid cells were determined as CD34$^-$/CD235a$^+$/SYTO16$^+$ and CD34$^-$/CD235a$^+$/SYTO16$^-$, respectively. The cells were interrogated using the BD LSR II flow cytometer and analyzed using FlowJo software.

Immunoblotting

Hemoglobin expression was analyzed by immunoblotting. Cells from cultures in hypoxia and normoxia were harvested on day 14, and $1-2 \times 10^5$ cells were lysed using RIPA buffer containing protease inhibitors and 1% Benzonase. Proteins were separated on either 15% or 4%–20% sodium dodecyl sulfate–polyacrylamide gel electrophoresis (SDS–PAGE) gels (Bio-Rad, Hercules, CA, Catalog No. 4561094), transferred onto PVDF membrane, and probed with antibodies to α-hemoglobin (BioLegend, San Diego, CA, Catalog No. 864001), β-hemoglobin (Santa Cruz Biotechnology, Dallas, TX, SC-21757), and GAPDH (Thermo Fisher Scientific, Catalog No. MA5–15738), and secondary anti-mouse and antirabbit antibodies conjugated to Cy3 and Cy5 fluorophores antibodies, respectively (Thermo Fisher Scientific). Blots were visualized using a Typhoon FLA 9500 imager, and proteins were quantified by densitometric scanning using ImageQuant.

t-Distributed stochastic neighbor embedding analysis

t-Distributed stochastic neighbor embedding (tSNE) analysis was performed using FlowJo software (TreeStar) with default parameters (iterations = 1000, perplexity = 30). For each normoxic and hypoxic sample, ~10,000 events were recorded in the CD34⁻/Live gate. All individual flow cytometry standard (FCS) files for the normoxic and hypoxic samples were combined into two new FCS files using the concatenation tool. Each concatenated FCS file was randomly downsampled to 18,000 events, and the tSNE analysis was run on an equal number of events per condition. The cell populations represented on the tSNE plots correspond to the respective gates drawn in the original FlowJo analysis. Both normoxia and hypoxia tSNE plots were generated from the same experimental data set.

Statistical analysis

All experiments, in both normoxia and hypoxia, were performed at least four times, and data are represented as the mean with standard error. For all experiments, data for hypoxia were compared with those for normoxia on each day of analysis. Statistical analysis was performed in GraphPad Prism Version 8.2 using the Mann-Whitney test, and a p value < 0.05 was considered statistically significant.

Results

Hypoxia reduces expansion of HSPCs and alters their metabolic profile

To examine the consequences of a hypoxic environment on proliferation and myeloerythroid differentiation of human CD34⁺ HSPCs, we chose 1% oxygen in our experiments to mimic the physiologic environment in bone marrow areas adjacent to the endosteal bone. CD34⁺ cells were isolated from CB and cocultured with mouse MS-5 stromal cells under normoxic (21% oxygen) and hypoxic (1% oxygen) conditions (Supplementary Figure E1, online only, available at www.exphem.org). We had previously optimized these coculture conditions for myeloerythroid differentiation in normal oxygen [28,29]. In addition to CD34, CD133 (also known as prominin-1) has been described as a stem cell marker in CB [40]. Weekly analysis of the Lin⁻/Live cells revealed that both CD34⁺ and CD133⁺ cells expanded significantly more in normoxia than in hypoxia; there was a ~30-fold increase in the number of CD34⁺

and CD133+ cells in normoxia versus a ~4-fold increase in hypoxia (Figure 1A,B). The percentage of CD34+ cells declined during the course of culture under both conditions; however, the rate of decrease in hypoxia was slower than that in normoxia (Figure 1C). Representative scatterplots that were used to calculate the positive populations are provided in Supplementary Figure E2 (online only, available at www.exphem.org).

To further characterize the CD34+ cell cultures, we examined the metabolites consumed and released into the medium by mass spectrometry (MS). Metabolite levels in the fresh medium were used to calculate fold change in spent medium on day 4 of culture. In principal component analysis and unsupervised hierarchical clustering on the basis of fold change, the samples clustered by treatment, thereby indicating similar metabolic properties of the biological replicates in hypoxia and normoxia (Figure 2A; Supplementary Figure E3, online only, available at www.exphem.org). A total of 135 metabolites were detected in MS analysis of the CD34+ cell cocultures (Supplementary Table E1, online only, available at www.exphem.org). Of these, levels of 82 and 70 changed significantly ($p < 0.05$, $n = 6$) relative to fresh medium in normoxia and hypoxia, respectively (Supplementary Tables E3 and E4, online only, available at www.exphem.org). Comparison of the metabolite profiles identified 57 that exhibited significantly different levels between normoxia and hypoxia (Supplementary Figure E3B and Supplementary Table E5, online only, available at www.exphem.org). Examination of supernatants from cultures of MS-5 cells alone also identified 135 metabolites (Supplementary Table E2, online only, available at www.exphem.org); however, no significant differences were observed in their levels between normoxia and hypoxia (Supplementary Table E6, online only, available at www.exphem.org). The MS-5 cultures incubated in normoxia or hypoxia did not cluster together (Supplementary Figure E4A, online only, available at www.exphem.org). They did not exhibit significant differences between the consumption of glucose, lactate, or amino acids in hypoxia and normoxia (Supplementary Figure E4B,C, online only, available at www.exphem.org). These observations suggest that on day 4 of analysis, the metabolic activity of MS-5 cells is low compared to that of the CD34+ cells and it is not very different between normoxia and hypoxia. Any significant differences in the metabolite levels in spent medium from cocultures are likely due to the CD34+ cells.

In spite of the low proliferation rate, glucose consumption by the CD34+ HSPCs was higher in hypoxia than in normoxia (Figure 2B). Extracellular levels of lactate were inversely correlated: higher in hypoxia than in normoxia. This indicates an upregulation of anaerobic glycolysis at low oxygen and reduced dependence of the CD34+ HSPCs on oxidative phosphorylation for ATP production in hypoxia. Several nonessential amino acids that can be synthesized by mammalian cells were found to be secreted in both hypoxia and normoxia (Figure 2C). These included asparagine, alanine, proline, aspartate, glutamate, glycine, and tyrosine. Glutamine and essential amino acids, including tryptophan, leucine, and isoleucine, were consumed more in normoxia than in hypoxia, indicating higher protein biosynthesis in proliferating cells. Compared with fresh medium, methionine and serine were consumed in both normoxia and hypoxia. Interestingly, serine was the only nonessential amino acid consumed; however, its consumption was significantly greater in hypoxia than in normoxia. More consumption of choline in normoxia indicates higher phospholipid biosynthesis in the proliferating CD34+ cells (Supplementary Figure E3B, online only, available at

www.exphem.org). Overall, these results indicated that in normoxia, the CD34^{+} HSPCs exhibit metabolic characteristics of proliferating cells. In low oxygen, reduction in proliferation is accompanied by altered metabolism; however, compared with normal oxygen, the stem cell phenotype is maintained.

Hypoxia promotes development of megakaryoerythroid progenitors

To assess the effect of hypoxic conditions on progenitor cells, we analyzed four subpopulations: multipotent progenitors (MPPs: CD34^{+}/CD38^{+}), the common myeloid progenitors (CMPs: CD34^{+}/CD38^{+}/CD123^{lo}/CD45RA^{−}), the granulomonocytic progenitors (GMPs: CD34^{+}/CD38^{+}/CD123^{lo}/CD45RA^{+}), and the megakaryoerythroid progenitors (MEPs: CD34^{+}/CD38^{+}/CD123^{−}/CD45RA^{−}) (Figure 3A). We examined the distribution of these populations using conventional flow cytometry scatterplots and t-Distributed Stochastic Neighbor Embedding (tSNE) analysis. Scatterplots depicting the gating strategy used for the estimation of populations and fold change in percentage of positive cells are provided in Supplementary Figure E5 (online only, available at www.exphem.org). Weekly analysis revealed that relative to normoxia, the fraction of MPPs and CMPs was significantly higher in hypoxia (Figure 3B). By day 7, there was an ~10-fold increase in the percentage of CMPs in hypoxia compared with ~2-fold in normoxia (Supplementary Figure E5B, online only, available at www.exphem.org). Although fold increase in the percentage positive cells is not very high in the case of MPPs and MEPs, their higher percentages in hypoxia combined with a decrease in normoxia suggest that hypoxia may be promoting their development to maintain the higher frequencies. These comparisons also reveal that the differentiation potential of CMPs is significantly different in hypoxia and normoxia. Cultures in hypoxia have a higher percentage of MEPs, whereas cultures in normoxia have a higher percentage of GMPs. Thus, hypoxic conditions may be altering the differentiation potential of CMPs toward the megakaryoerythroid lineage.

For tSNE analysis, individual flow cytometry standard files were concatenated into a single file, and cell populations identified by conventional gating strategies were overlaid onto tSNE plots. Overlaying the CD34^{+} and CD38^{+} gates onto Lin^{−}/Live cells revealed the double-positive populations and the expected difference in the percentage of MPPs in hypoxia and normoxia (Figure 3C). The tSNE plots revealed that the CD34^{+}/CD38^{+} MPPs were higher in hypoxia than in normoxia. Similarly, overlaying the progenitor gates onto the CD34^{+}/CD38^{+} population tSNE plots indicated a higher percentage of CMPs and MEPs and a lower percentage of GMP in hypoxia than in normoxia (Figure 3D). The histograms for CD123 and CD45RA further confirmed the characteristics of each population (Figure 3E). They illustrated that the CD123^{−}/CD45RA^{+} GMPs were fewer in hypoxia than in normoxia. The CD123^{+}/CD45RA^{+} CMPs and CD123^{−}/CD45RA^{−} MEPs, on the other hand, were both higher in hypoxia. Thus, these analyses revealed that low-oxygen conditions may be supporting the maintenance of MPP, CMP, and MEP levels in culture.

Low oxygen increases erythroid differentiation

To monitor the lineage cells, we immunophenotyped the CD34^{−} population with markers for monocytes (CD14), granulocytes (CD66b), megakaryocytes (CD41a) and erythrocytes (CD235a/glycophorin A) on days 14 and 21. This analysis revealed that the fraction of

erythroid cells (CD34⁻/CD41a⁻/CD235a⁺) was significantly higher in hypoxia (Figure 4A). This increase was accompanied by a concomitant decrease in granulocytes (CD34⁻/CD14⁻/CD66b⁺) and megakaryocytes (CD34⁻/CD41a⁺/CD235a⁻) but not a significant effect on the fraction of monocytes (CD34⁻/CD14⁺/CD66b⁻). Representative scatterplots that were used to calculate the lineage cells are provided in Supplementary Figure E6 (online only, available at www.exphem.org).

Because low oxygen did not significantly affect the development of monocytes, we examined if expression of myeloid precursors markers CD33 and CD11b was altered. CD33, a sialic acid-binding immunoglobulin-like lectin (also known as Siglec-3), is an early marker in myeloid cell development. It first appears on CD34⁺ CFU-GEMM cells and is expressed by myeloblasts and monoblasts, granulocyte precursors, and mature monocytes, and may be expressed by mature granulocytes at a very low level [41]. CD11b is expressed by mature granulocytes and monocytes. Both are not expressed on erythroid and megakaryocytic cells. Representative scatterplots that were used to calculate the positive populations are provided in Supplementary Figure E7 (online only, available at www.exphem.org). We observed a steady decline in CD33⁺ cells in hypoxia, whereas an initial drop on day 7 was followed by an increase on days 14 and 21 in normoxia (Figure 4B). There was a rapid decline in the percentage of CD34⁺/CD33⁺ cells in normoxia and hypoxia, the rate of decrease being slower in hypoxia. The CD34⁻/CD33⁺ cells increased until day 14 in both conditions and, thereafter, continued to rise in normoxia, but not in hypoxia. The CD11b⁺ cells increased in both conditions, with the rate being higher in hypoxia (Figure 4C). This increase was due largely to a rise in the CD34⁻/CD11b⁺ cells. The CD34⁺/CD11b⁺ cells were low in both culture conditions. Thus, these observations suggest that in hypoxia, there may be a decline in CD33⁺ myeloid progenitors but an increase in CD11b⁺ precursor cells. Overall, the analysis of lineage markers revealed that enhanced erythroid differentiation in low oxygen was accompanied by a significant decrease in granulocytes and megakaryocytes, but monocytes were not affected.

Hypoxia enhances formation of CD235a⁺ erythroid cells

To further elucidate the influence of hypoxia on erythropoiesis, we monitored the expression of erythroid markers, CD71, CD235a, and CD239. CD71 (transferrin receptor) is expressed in erythroid cells at all stages of development, but is absent from mature erythrocytes [42–45]. CD235a (glycophorin A) and CD239 (Lutheran glycoprotein antigen), on the other hand, are highly expressed in the mature erythrocytes. Analysis of these markers in the CD34⁻ population revealed an initial increase in the fraction of cells expressing CD71 on day 7, followed by a decline on days 14 and 21 in normoxia (Supplementary Figure E8A, online only, available at www.exphem.org). In hypoxia, there was a steady decline in the CD71⁺ cells during the course of the experiment. There was an increase in the fractions of CD235a⁺ and CD239⁺ cells in normoxia and hypoxia. However, the percentage of positive cells was significantly higher in hypoxia than in normoxia, thereby indicating that the rate of increase might be greater in hypoxia. Representative scatterplots used to calculate positive populations are provided in Supplementary Figure E8B and E8C (online only, available at www.exphem.org).

Comparison of CD71 expression relative to that of CD235a and CD239 revealed that hypoxia enhanced erythroid maturation. Weekly analysis of cells in the CD34$^-$ compartment indicated a clear transition in from CD71$^+$/CD235a$^-$ and CD71$^+$/CD239$^-$ cells to CD71$^-$/CD235a$^+$ and CD71$^-$/CD239$^+$ cells, respectively, in normoxia and hypoxia; there was a progressive decrease in the CD71$^+$ cells and parallel increase in the CD235$^+$ and CD239$^+$ erythroid cells (Figure 5A, B). The percentages of CD71$^+$/CD235a$^-$ and CD71$^+$/CD239$^-$ cells were significantly lower, and those of CD71$^-$/CD235a$^+$ and CD71$^-$/CD239$^+$ erythroid cells were significantly higher in hypoxia than in normoxia, indicating that the transition to erythroid cells was accelerated in hypoxia. The double-positive intermediate populations (CD71$^+$/CD235a$^+$ and CD71$^+$/CD239$^+$) were low and not found to differ significantly between hypoxia and normoxia. Further, the CD235a$^+$/CD239$^+$ double-positive cells increased significantly in hypoxia compared with normoxia (Supplementary Figure E9, online only, available at www.exphem.org). Representative scatterplots used to calculate positive populations are provided in Supplementary Figure E8D (online only, available at www.exphem.org). Visualization of the cellular phenotypes using tSNE maps revealed similar trends. On day 21, the CD71$^+$ cells were lower and the CD235a$^+$ and CD239$^+$ cells were higher in hypoxia than in normoxia (Figure 5C, compare normoxia and hypoxia plots). Overlays of the single-positive populations revealed lower numbers of double-positive cells (CD71$^+$/CD235a$^+$ and CD71$^+$/CD239$^+$) and higher numbers of erythroid cells (CD71$^-$/CD235a$^+$ and CD71$^-$/CD239$^+$) in hypoxia than in normoxia (Figure 5D).

Hypoxia promotes formation of proerythroblasts

CD105 (endoglin) has been described as an erythroblast marker that is expressed in ProE and BasoE, which also express CD235a [45,46]. In early erythroblasts, CD105 expression precedes that of CD71 and CD235a. In the CD34$^-$ population, the fraction of CD105$^+$ cells increased, with no significant difference between normoxia and hypoxia (Supplementary Figure E8A, online only, available at www.exphem.org). Examination of CD105 relative to CD71 and CD235a in the CD34$^-$ population revealed an increase in CD105$^+$/CD71$^-$ and CD105$^+$/CD235a$^-$ in both normoxia and hypoxia at later points in culture (Figure 6A,B). During the course of culture, the levels of CD105$^+$/CD71$^-$ cells did not differ significantly between normoxia and hypoxia. The percentage of CD71$^+$/CD105$^+$ cells remained low in both normoxia and hypoxia, indicating lack of accumulation of the double-positive population in either condition. A decline in CD71$^+$/CD105$^-$ cells was observed in both normoxia and hypoxia, with the rate of decrease being faster in hypoxia than in normoxia, once again indicating enhanced erythroid maturation in hypoxia (Figure 6A). The increase in CD105$^+$/CD235a$^-$ cells on day 14 was followed by a significant decrease in hypoxia, but not in normoxia on day 21 (Figure 6B). The percentage of the CD105$^-$/CD235a$^+$ cells did not significantly differ between hypoxia and normoxia; however, the CD105$^+$/CD235a$^+$ cells increased significantly in hypoxia in comparison with normoxia, indicating that there may be enhancement of this population in hypoxia. The tSNE plots confirm the presence of similar numbers of CD105$^+$ cells in hypoxia and normoxia (Figure 6C). They also indicate higher levels of CD105$^+$/CD235a$^+$ cells in hypoxia than in normoxia. Thus, the results indicated a rise in CD105$^+$ cells and its sustained expression at later time points in both hypoxia and normoxia. The presence of significantly higher levels of CD105$^+$/CD235a$^+$

cells in hypoxia suggests that the hypoxic conditions were enhancing formation of ProE and/or BasoE.

A combination of CD49d (α4 integrin) and CD233 (band 3) has been previously employed to distinguish the erythroblast stages in the CD235a$^+$ population [26]. In these studies, CD49d was found to be expressed in ProE, BasoE, PolyE, OrthoE, and reticulocytes, whereas CD233 expression was found to begin in BasoE and continued to increase with erythroid maturation [26]. Thus, ProEs were considered to be CD49d$^+$/CD233$^-$, and BasoE, PolyE, OrthoE, and reticulocytes were reported to be CD49d$^+$/CD233$^+$ with varying levels of CD49d and CD233 expression. During the course of culture, we found that within the CD235a$^+$ population, the fraction of CD49d$^+$ cells declined and CD233$^+$ cells increased; however, there was not a significant difference between the hypoxia and normoxia conditions (Supplementary Figure E10, online only, available at www.exphem.org). Further, within the CD235a$^+$ population, the fractions of CD49d$^+$/CD233$^-$, CD49d$^+$/CD233$^+$, and CD49d$^-$/CD233$^+$ cells also did not differ significantly between hypoxia and normoxia (Figure 6D). However, we observed that the percentage of CD235a$^+$ cells that were CD49d$^-$/CD233$^-$ was significantly higher in hypoxia than in normoxia. This indicated that hypoxia was enhancing the expression of CD235a, but the acquisition of CD49d and CD233 in the CD235a$^+$ cells occurred at similar rates in hypoxia and normoxia. Representative scatterplots that were used to calculate positive populations are provided in Supplementary Figure E10B and E10C (online only, available at www.exphem.org). Put together, the erythroblast marker analysis revealed that hypoxic conditions promoted the CD235a$^+$/CD49d$^-$/CD233$^-$ and CD105$^+$/CD235a$^+$ cells, thereby indicating a hypoxia-induced enhancement in the formation of ProEs during ex vivo differentiation of human HSPCs. The lack of a difference in CD49d$^+$/CD233$^-$, CD49d$^+$/CD233$^+$, and CD49d$^-$/CD233$^+$ in normoxia versus hypoxia suggests that intermediate stages, BasoE, OrthoE, and PolyE are likely not affected.

Hypoxia promotes enucleation of erythroid cells

During erythroid differentiation, expression of hemoglobin begins in ProEs and continues to rise during maturation. To determine if hypoxia was affecting hemoglobin expression, we harvested the cells on day 14 of culture and performed immunoblotting. Probing with antibodies to α- and β-hemoglobin did not reveal a significant difference in expression between hypoxia and normoxia (Figure 7A). To examine if enhanced erythroid maturation in hypoxia was accompanied by enucleation, we used the live cell nuclear stain SYTO16 and monitored changes in the levels of CD235a$^+$/SYTO16$^+$ and CD235a$^+$/SYTO16$^-$ cells. In normoxia, ~97% and ~92% of the cells were SYTO16$^+$ on days 14 and 21, respectively, indicating efficient staining and low enucleation (Figure 7B). In hypoxia, SYTO16$^+$ cells decreased to ~63% and ~43% on days 14 and 21, respectively. This decrease was accompanied by an increase in the percentage of CD235a$^+$/SYTO16$^-$ cells, thereby indicating increased enucleation of the erythroid cells in hypoxia (Figure 7C). The lack of accumulation of enucleated cells likely indicates that there is not a significant increase in enucleation after day 14 or that there may be some loss of enucleated cells during culture and/or staining. The CD235a$^+$/SYTO16$^+$ cells were significantly lower on days 14 and 21 in hypoxia than in normoxia, indicating that they may be an intermediate population. Overall,

the results indicated that low oxygen does not affect the expression of α- and β-hemoglobin but promotes the enucleation of CD235a$^+$ erythroid cells.

Discussion

Our study was designed to examine how hypoxic microenvironment affects proliferation and myeloerythroid differentiation of human CD34$^+$ cells. We found that under the conditions used, the cultures were able to withstand low (1%) and normal (21%) oxygen tension for an extended time up to 3 weeks. In agreement with several previous reports, we observed a dramatic inhibition of expansion of the CD34$^+$ and CD133$^+$ cells at low but not at normal oxygen [13,47,48]. Notably, this phenomenon has been reported to not occur at an intermediate level of 5% oxygen, and additionally, incubation of cells under dynamic conditions (with shaking) was found to cause a higher fold expansion at 5% than at 20% [49]. The normoxia cultures exhibited characteristics of proliferating cells, including increased consumption of essential amino acids and choline. In hypoxia, there was an upregulation of anaerobic glycolysis and reduced dependence on oxidative phosphorylation for ATP production. Similar to previous studies, these results indicate metabolic adaptation by the CD34$^+$ cells in hypoxia [19].

Our analysis of the Lin$^-$/CD34$^+$ cells revealed a distinct distribution of the progenitor populations in normoxia and hypoxia. There was a hypoxia-associated maintenance of the fraction of MPPs and CMPs. In hypoxia, CMPs gave rise to more MEPs than GMPs. Erythroid differentiation progresses through multiple developmental stages, and MEPs are thought to precede CFU-Es and BFU-Es [50]. Studies using the conventional colony-forming assay for enumeration of CFU-Es and BFU-Es have obtained mixed results. Some have found a hypoxia-associated increase in BFU-Es and CFU-Es [14], whereas others have reported lack of an effect [13,24,51]. These discrepancies could be because of variations in composition and concentration of cytokines used in the CFU assays, as well as the length of hypoxia treatment and the percentage of oxygen used. Our findings suggest that further characterization of BFU-Es and CFU-Es using more recently described markers may be crucial to completely understand hypoxia-associated changes in erythroid progenitor phenotypes [52].

Under the conditions used in this study, MEPs in hypoxia preferentially differentiated into erythroid cells rather than megakaryocytes. This was also accompanied by a decrease in granulocytes but not in monocytes. Presence of monocytic cells has been reported in conditions of stress erythropoiesis [53]. Ablation of monocytic cells has been reported to compromise normal and stress erythropoiesis [54,55]. In our culture system, the increased expression of other myeloid and monocytic markers (CD33, CD11b, and CD14) may be indicative of a similar need for monocytes in hypoxic conditions.

In summary, immunophenotyping for progenitor and lineage markers revealed the extensive role of hypoxia during myeloerythroid differentiation. We found that in hypoxia, there was rapid loss of CD71 and a gain of CD235a and CD239, indicating an increase in erythroid differentiation. Further, analysis of the erythroblast markers suggested that hypoxia may be promoting formation of ProE, but may not influence the transition of

ProE→BasoE→OrthoE→PolyE. Finally, the hypoxic CD235a$^+$ erythroid cells exhibited an increase in enucleation. These findings represent a significant indication for further investigations into the relationship between erythroid progenitors/proerythroblasts and their hypoxic microenvironment for exploring cellular and metabolic events that may initiate normal and pathophysiological phenotypes.

Supplementary Material

Refer to Web version on PubMed Central for supplementary material.

Acknowledgments

References

1. Szade K, Gulati GS, Chan CKF, et al. Where hematopoietic stem cells live: the bone marrow niche. Antioxid Redox Signal. 2018;29:191–204. [PubMed: 29113449]

2. Garcia M, Chen CC. The bone marrow microenvironment—driver of leukemia evolution? Stem Cell Investig. 2017;4:11.

3. Calvi LM, Li AJ, Becker MW. What is the role of the microenvironment in MDS? Best Pract Res Clin Haematol. 2019;32:101113. [PubMed: 31779976]

4. Morrison SJ, Scadden DT. The bone marrow niche for haematopoietic stem cells. Nature. 2014;505:327–334. [PubMed: 24429631]

5. Crane GM, Jeffery E, Morrison SJ. Adult haematopoietic stem cell niches. Nat Rev Immunol. 2017;17:573–590. [PubMed: 28604734]

6. Yu VW, Scadden DT. Hematopoietic stem cell and its bone marrow niche. Curr Top Dev Biol. 2016;118:21–44. [PubMed: 27137653]

7. Spencer JA, Ferraro F, Roussakis E, et al. Direct measurement of local oxygen concentration in the bone marrow of live animals. Nature. 2014;508:269–273. [PubMed: 24590072]

8. Parmar K, Mauch P, Vergilio JA, Sackstein R, Down JD. Distribution of hematopoietic stem cells in the bone marrow according to regional hypoxia. Proc Natl Acad Sci USA. 2007;104:5431–5436. [PubMed: 17374716]

9. Kobayashi H, Morikawa T, Okinaga A, et al. Environmental optimization enables maintenance of quiescent hematopoietic stem cells ex vivo. Cell Rep. 2019;28. 145–158.e149. [PubMed: 31269436]

10. Mantel CR, O'Leary HA, Chitteti BR, et al. Enhancing hematopoietic stem cell transplantation efficacy by mitigating oxygen shock. Cell. 2015;161:1553–1565. [PubMed: 26073944]

11. Hammoud M, Vlaski M, Duchez P, et al. Combination of low O2 concentration and mesenchymal stromal cells during culture of cord blood CD34(+) cells improves the maintenance and proliferative capacity of hematopoietic stem cells. J Cell Physiol. 2012;227:2750–2758. [PubMed: 21913190]

12. Shima H, Takubo K, Iwasaki H, et al. Reconstitution activity of hypoxic cultured human cord blood CD34-positive cells in NOG mice. Biochem Biophys Res Commun. 2009;378:467–472. [PubMed: 19032938]

13. Danet GH, Pan Y, Luongo JL, Bonnet DA, Simon MC. Expansion of human SCID-repopulating cells under hypoxic conditions. J Clin Invest. 2003;112:126–135. [PubMed: 12840067]

14. Vlaski M, Lafarge X, Chevaleyre J, Duchez P, Boiron JM, Ivanovic Z. Low oxygen concentration as a general physiologic regulator of erythropoiesis beyond the EPO-related downstream tuning

and a tool for the optimization of red blood cell production ex vivo. Exp Hematol. 2009;37:573–584. [PubMed: 19375648]

15. Cipolleschi MG, D'Ippolito G, Bernabei PA, et al. Severe hypoxia enhances the formation of erythroid bursts from human cord blood cells and the maintenance of BFU-E in vitro. Exp Hematol. 1997;25:1187–1194. [PubMed: 9328456]

16. Koller MR, Bender JG, Miller WM, Papoutsakis ET. Reduced oxygen tension increases hematopoiesis in long-term culture of human stem and progenitor cells from cord blood and bone marrow. Exp Hematol. 1992;20:264–270. [PubMed: 1544397]

17. Suda T, Takubo K, Semenza GL. Metabolic regulation of hematopoietic stem cells in the hypoxic niche. Cell Stem Cell. 2011;9:298–310. [PubMed: 21982230]

18. Jang YY, Sharkis SJ. A low level of reactive oxygen species selects for primitive hematopoietic stem cells that may reside in the low-oxygenic niche. Blood. 2007;110:3056–3063. [PubMed: 17595331]

19. Simsek T, Kocabas F, Zheng J, et al. The distinct metabolic profile of hematopoietic stem cells reflects their location in a hypoxic niche. Cell Stem Cell. 2010;7:380–390. [PubMed: 20804973]

20. Oburoglu L, Tardito S, Fritz V, et al. Glucose and glutamine metabolism regulate human hematopoietic stem cell lineage specification. Cell Stem Cell. 2014;15:169–184. [PubMed: 24953180]

21. Ito K, Carracedo A, Weiss D, et al. A PML-PPAR-delta pathway for fatty acid oxidation regulates hematopoietic stem cell maintenance. Nat Med. 2012;18:1350–1358. [PubMed: 22902876]

22. Manz MG, Miyamoto T, Akashi K, Weissman IL. Prospective isolation of human clonogenic common myeloid progenitors. Proc Natl Acad Sci USA. 2002;99:11872–11877. [PubMed: 12193648]

23. Parekh C, Sahaghian A, Kim W, et al. Novel pathways to erythropoiesis induced by dimerization of intracellular C-Mpl in human hematopoietic progenitors. Stem Cells. 2012;30:697–708. [PubMed: 22290824]

24. Zhou L, Zhang X, Zhou P, et al. Effect of testosterone and hypoxia on the expansion of umbilical cord blood CD34(+) cells in vitro. Exp Ther Med. 2017;14:4467–4475. [PubMed: 29067121]

25. Rogers HM, Yu X, Wen J, Smith R, Fibach E, Noguchi CT. Hypoxia alters progression of the erythroid program. Exp Hematol. 2008;36:17–27. [PubMed: 17936496]

26. Hu J, Liu J, Xue F, et al. Isolation and functional characterization of human erythroblasts at distinct stages: implications for understanding of normal and disordered erythropoiesis in vivo. Blood. 2013;121:3246–3253. [PubMed: 23422750]

27. Ivanovic Z, Hermitte F, Brunet de la Grange P, et al. Simultaneous maintenance of human cord blood SCID-repopulating cells and expansion of committed progenitors at low O$_2$ concentration (3%). Stem Cells. 2004;22:716–724. [PubMed: 15342936]

28. Bapat A, Keita N, Martelly W, et al. Myeloid disease mutations of splicing factor SRSF2 cause G2-M arrest and skewed differentiation of human hematopoietic stem and progenitor cells. Stem Cells. 2018;36:1663–1675. [PubMed: 30004607]

29. Bapat A, Keita N, Sharma S. Pan-myeloid differentiation of humancord blood derived CD34+ hematopoietic stem and progenitor cells. J Vis Exp. 2019;150. 10.3791/59836.

30. Jasbi P, Mitchell NM, Shi XJ, et al. Coccidioidomycosis detection using targeted plasma and urine metabolic profiling. J Proteome Res. 2019;18:2791–2802. [PubMed: 31244214]

31. Zhu J, Djukovic D, Deng L, et al. Colorectal cancer detection using targeted serum metabolic profiling. J Proteome Res. 2014;13:4120–4130. [PubMed: 25126899]

32. Carroll PA, Diolaiti D, McFerrin L, et al. Deregulated Myc requires MondoA/Mlx for metabolic reprogramming and tumorigenesis. Cancer Cell. 2015;27:271–285. [PubMed: 25640402]

33. Gu H, Zhang P, Raftery D. Globally optimized targeted mass spectrometry (GOT-MS): Reliable metabolomics analysis with broad coverage. Anal Chem. 2015;87:12355–12362. [PubMed: 26579731]

34. Gu H, Carroll PA, Du J, et al. Quantitative method to investigate the balance between metabolism and proteome biomass: Starting from glycine. Angew Chem Int Ed Engl. 2016;55:15646–15650. [PubMed: 27860107]

35. Li RF, Grimm SA, Mav D, et al. Transcriptome and DNA methylome analysis in a mouse model of diet-induced obesity predicts increased risk of colorectal cancer. Cell Rep. 2018;22:624–637. [PubMed: 29346762]

36. Buas MF, Gu HW, Djukovic D, et al. Candidate serum metabolite biomarkers for differentiating gastroesophageal reflux disease, Barrett's esophagus, and high-grade dysplasia/esophageal adenocarcinoma. Metabolomics. 2017;13:23. [PubMed: 28190989]

37. Jasbi P, Wang DF, Cheng SL, et al. Breast cancer detection using targeted plasma metabolomics. J Chromatogr B Analyt Technol Biomed Life Sci. 2019;1105:26–37.

38. Shi XJ, Wang S, Jasbi P, et al. Database-assisted globally optimized targeted mass spectrometry (dGOT-MS): Broad and reliable metabolomics analysis with enhanced identification. Anal Chem. 2019;91:13737–13745. [PubMed: 31556994]

39. Wlodkowic D, Skommer J, Darzynkiewicz Z. Rapid quantification of cell viability and apoptosis in B-cell lymphoma cultures using cyanine SYTO probes. Methods Mol Biol. 2011;740:81–89. [PubMed: 21468970]

40. Sumide K, Matsuoka Y, Kawamura H, et al. A revised road map for the commitment of human cord blood CD34-negative hematopoietic stem cells. Nat Commun. 2018;9:2202. [PubMed: 29875383]

41. Naeim F, Rao PN, Song SX, Phan RT. Atlas of hematopathology. San Diego, CA: Academic Press; 2018. p. 29–56.

42. Machherndl-Spandl S, Suessner S, Danzer M, et al. Molecular pathways of early CD105-positive erythroid cells as compared with CD34-positive common precursor cells by flow cytometric cell-sorting and gene expression profiling. Blood Cancer J. 2013;3:e100. [PubMed: 23310930]

43. Marsee DK, Pinkus GS, Yu H. CD71 (transferrin receptor): an effective marker for erythroid precursors in bone marrow biopsy specimens. Am J Clin Pathol. 2010;134:429–435. [PubMed: 20716799]

44. Dong HY, Wilkes S, Yang H. CD71 is selectively and ubiquitously expressed at high levels in erythroid precursors of all maturation stages: a comparative immunochemical study with glycophorin A and hemoglobin A. Am J Surg Pathol.2011;35:723–732. [PubMed: 21415701]

45. Wangen JR, Eidenschink Brodersen L, Stolk TT, Wells DA, Loken MR. Assessment of normal erythropoiesis by flow cytometry: important considerations for specimen preparation. Int J Lab Hematol. 2014;36:184–196. [PubMed: 24118926]

46. Fajtova M, Kovarikova A, Svec P, Kankuri E, Sedlak J. Immunophenotypic profile of nucleated erythroid progenitors during maturation in regenerating bone marrow. Leuk Lymphoma. 2013;54:2523–2530. [PubMed: 23452116]

47. Guitart AV, Hammoud M, Dello Sbarba P, Ivanovic Z, Praloran V. Slow-cycling/quiescence balance of hematopoietic stem cells is related to physiological gradient of oxygen. Exp Hematol. 2010;38:847–851. [PubMed: 20547202]

48. Eliasson P, Rehn M, Hammar P, et al. Hypoxia mediates low cell-cycle activity and increases the proportion of long-term-reconstituting hematopoietic stem cells during in vitro culture. Exp Hematol. 2010;38:301–310.e302. [PubMed: 20138114]

49. Tiwari A, Wong CS, Nekkanti LP, et al. Impact of oxygen levels on human hematopoietic stem and progenitor cell expansion. Stem Cells Dev. 2016;25:1604–1613. [PubMed: 27539189]

50. Dzierzak E, Philipsen S. Erythropoiesis: development and differentiation. Cold Spring Harb Perspect Med. 2013;3:a011601. [PubMed: 23545573]

51. Zhao D, Liu L, Chen Q, et al. Hypoxia with Wharton's jelly mesenchymal stem cell coculture maintains stemness of umbilical cord blood-derived CD34(+) cells. Stem Cell Res Ther. 2018;9:158. [PubMed: 29895317]

52. Li J, Hale J, Bhagia P, et al. Isolation and transcriptome analyses of human erythroid progenitors: BFU-E and CFU-E. Blood. 2014;124:3636–3645. [PubMed: 25339359]

53. Xiang J, Wu DC, Chen Y, Paulson RF. In vitro culture of stress erythroid progenitors identifies distinct progenitor populations and analogous human progenitors. Blood. 2015;125:1803–1812. [PubMed: 25608563]

54. Chow A, Huggins M, Ahmed J, et al. CD169(+) macrophages provide a niche promoting erythropoiesis under homeostasis and stress. Nat Med. 2013;19:429–436. [PubMed: 23502962]

55. Ramos P, Casu C, Gardenghi S, et al. Macrophages support pathological erythropoiesis in polycythemia vera and beta-thalassemia. Nat Med. 2013;19:437–445. [PubMed: 23502961]
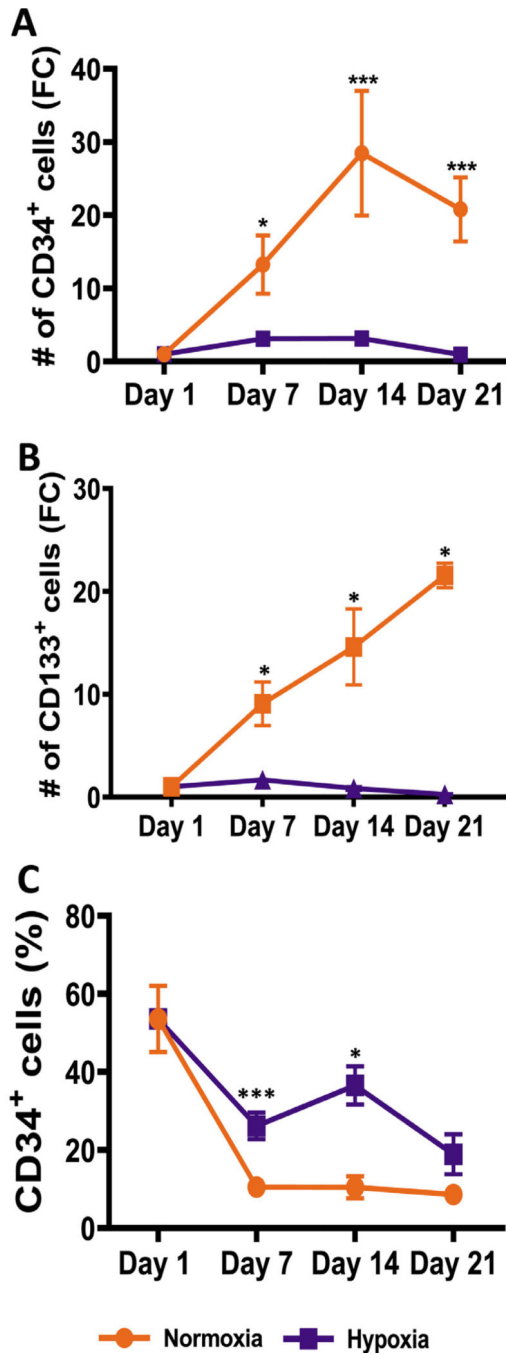
Figure 1.
Hypoxia reduces proliferation of CD34^{+} hematopoietic stem and progenitor cells. CD34^{+} and CD133^{+} cells in cultures in both hypoxia and normoxia were determined by flow cytometry on days 1, 7, 14 and 21. **(A)** Fold change in the number of CD34^{+} cells in the normoxic and hypoxic cultures was calculated relative to day 1. **(B)** Fold change in the number of CD133^{+} cells in the normoxic and hypoxic cultures was calculated relative to day 1. **(C)** Percentage of CD34^{+} cells in the Lin^{−}/Live population is shown. Data are represented as the mean with standard error ($n = 6$ for CD34 and $n = 4$ for CD133). Statistical analysis

was performed using the Mann-Whitney test, and p values ≤ 0.05 were considered significant. $*p < 0.05$, $**p < 0.005$, $***p < 0.0005$.
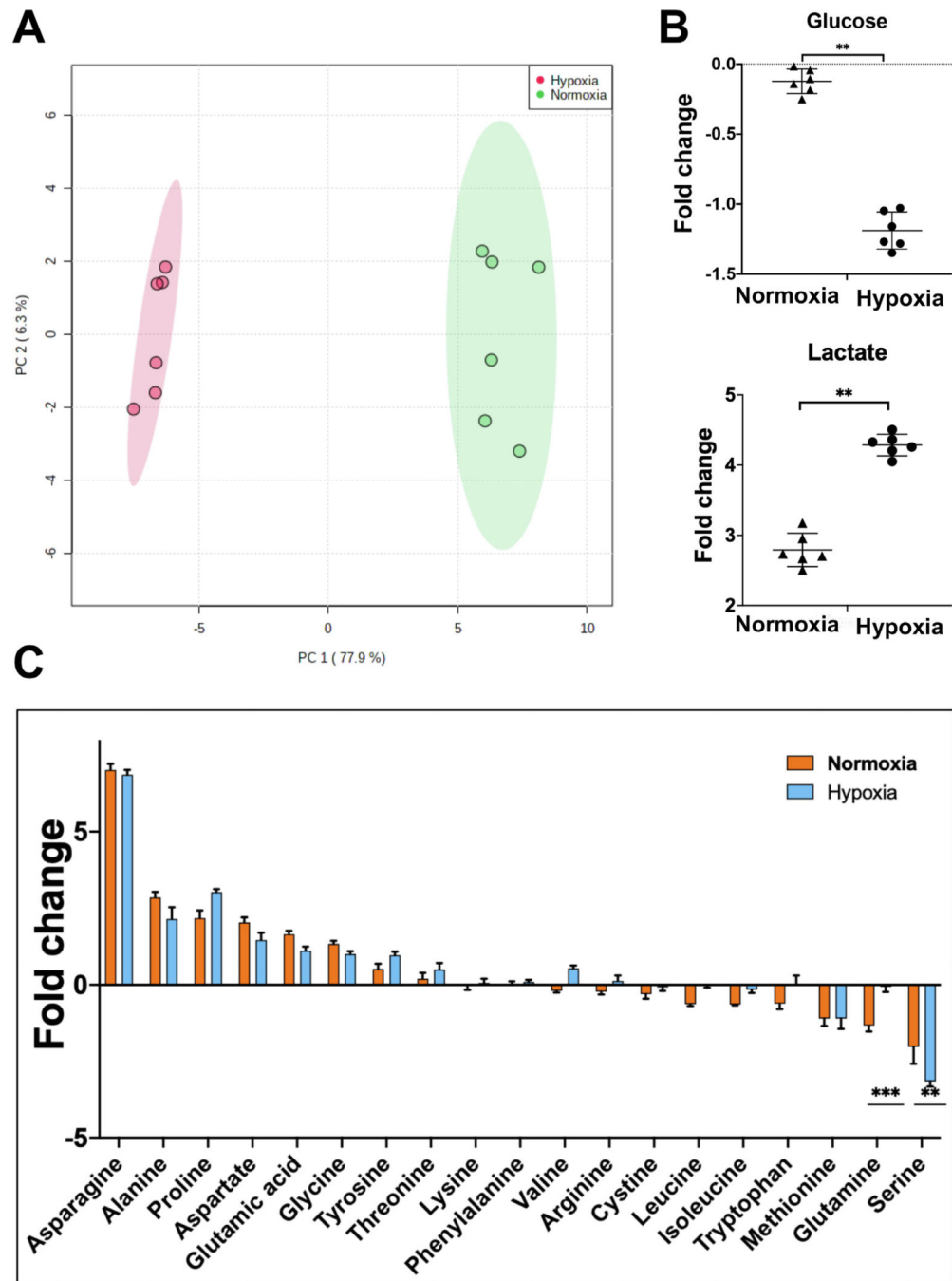
Figure 2.
Hypoxia causes a metabolic shift in CD34^{+} hematopoietic stem and progenitor cells. **(A)** Principal component analysis of samples on the basis of fold change in metabolites in spent medium relative to fresh medium from CD34^{+} cell cultures incubated in hypoxia or normoxia. **(B)** Fold change in glucose and lactate in spent medium relative to fresh medium from CD34^{+} cell cultures incubated in normoxia or hypoxia. **(C)** Fold change in amino acids in spent medium relative to fresh medium from CD34^{+} cell cultures incubated in normoxia or hypoxia. Spent medium was collected on day 4 of culture. Statistical analysis was

performed in MetaboAnalyst, and p values ≤ 0.05 were considered significant. $*p < 0.05$, $**p < 0.005$, $***p < 0.0005$.
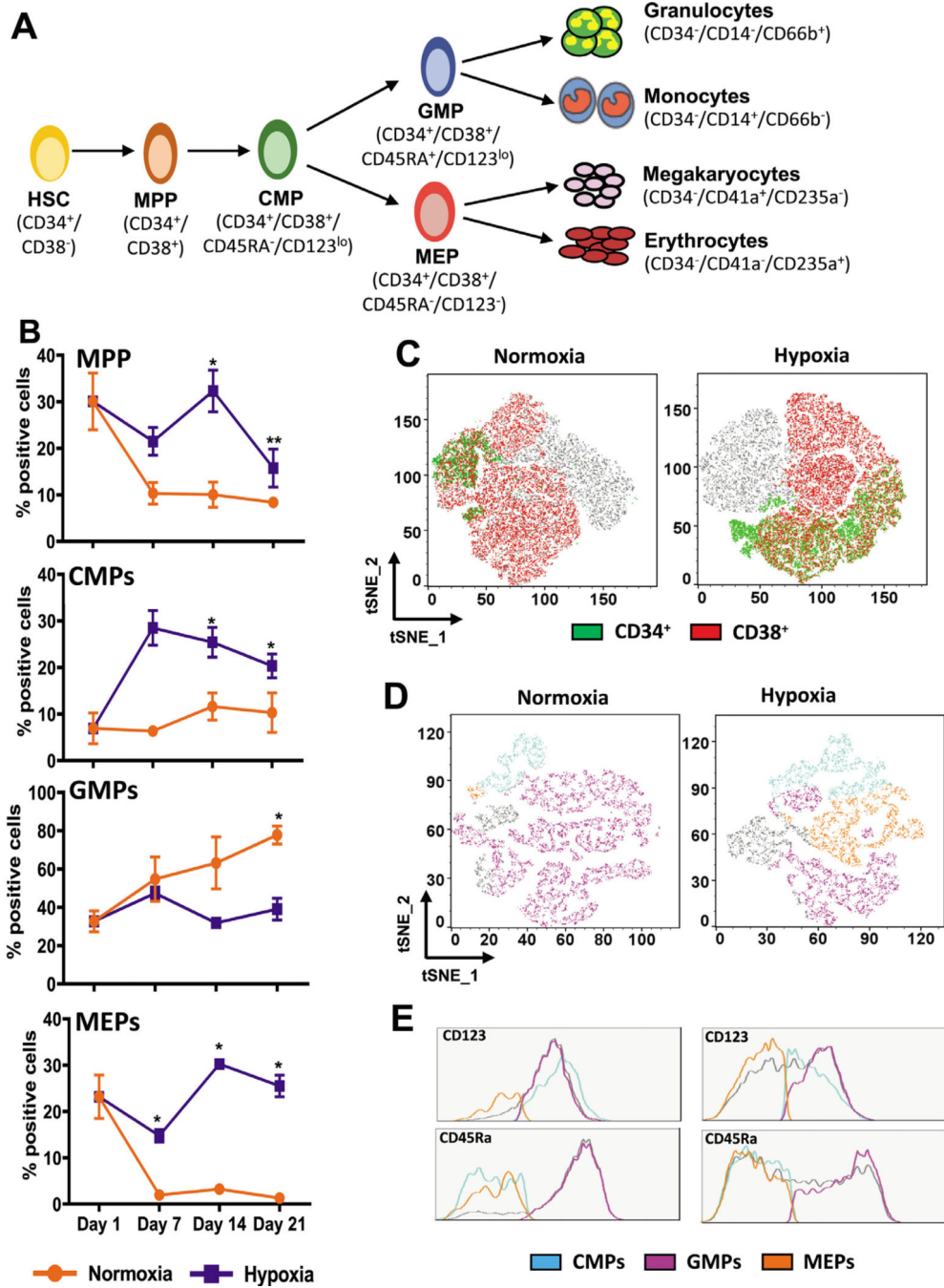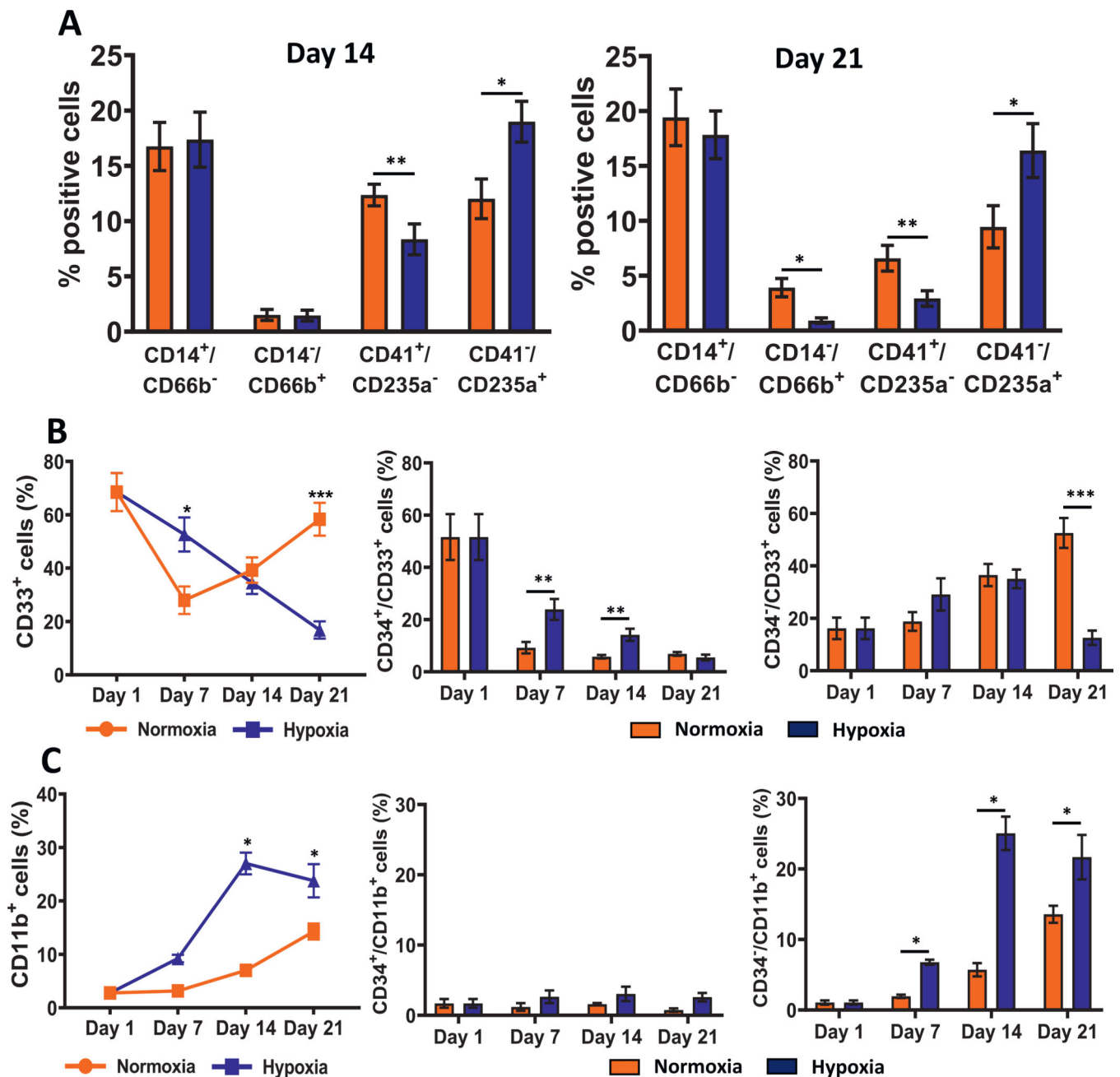
Figure 3.

Hypoxia promotes the development of megakaryoerythroid progenitors. **(A)** Schematic of myeloerythroid differentiation from hematopoietic stem cells. The surface markers used for immunophenotyping of the cells interrogated in this study are indicated. **(B)** Percentage of multipotent progenitors (MPP), common myeloid progenitors (CMP), megakaryoerythroid progenitors (MEP), and granulocyte–monocyte progenitors (GMP) in cultures incubated in hypoxia and normoxia. For MPPs, the percentage of positive cells in the Lin⁻/Live population was determined, and for CMPs, GMPs, and MEPs, the percentage of positive

cells in the MPP population was determined on days 1, 7, 14, and 21. Data are represented as the mean with standard error ($n = 4$). Statistical analysis was performed using the Mann-Whitney test, and p values 0.05 were considered significant. **(C)** tSNE analysis was performed on flow cytometry standard files. tSNE plots for day 21 analysis revealing CD34$^+$ and CD38$^+$ cells in normoxia and hypoxia are represented in the Lin$^-$/Live population. **(D)** tSNE analysis plots revealing the distribution of CMPs, GMPs, and MEPs in the CD34$^+$/CD38$^+$ population in normoxia or hypoxia on day 21 are represented. **(E)** Histograms for CD45Ra and CD123 expression indicating relative distribution of CMPs (CD45Ra$^-$/CD123^{lo}), GMPs (CD45Ra$^+$/CD123^{lo}), and MEPs (CD45Ra$^-$/CD123$^-$) in normoxia and hypoxia. $*p < 0.05$, $**p < 0.005$, $***p < 0.0005$.

Figure 4.

Hypoxia increases erythroid differentiation. **(A)** Immunophenotypic analysis of lineage cells: monocytes (CD34−/CD14+/CD66b−), granulocytes (CD34−/CD14−/CD66b+), megakaryocytes (CD34−/CD41a+/CD235a−), and erythrocytes (CD34−/CD41a−/CD235a+) on days 14 and 21. Percentage of positive cells in the CD34−/Live population are illustrated. **(B)** Distribution of cells expressing CD33 was determined on days 1, 7, 14, and 21 by flow cytometry. Percentages of total CD33+, CD34+/CD33+, and CD34−/CD33+ cells in the live population are illustrated. **(C)** Distribution of cells expressing CD11b was determined on days 1, 7, 14, and 21 by flow cytometry. Percentages of total CD11b+, CD34+/CD11b+, and

CD34$^-$/CD11b$^+$ cells in the live population are illustrated. Data are represented as the mean with standard error ($n = 4$). Statistical analysis was performed using the Mann-Whitney test, and p values $\leq$ 0.05 were considered significant. *$p < 0.05$, **$p < 0.005$, ***$p < 0.0005$.
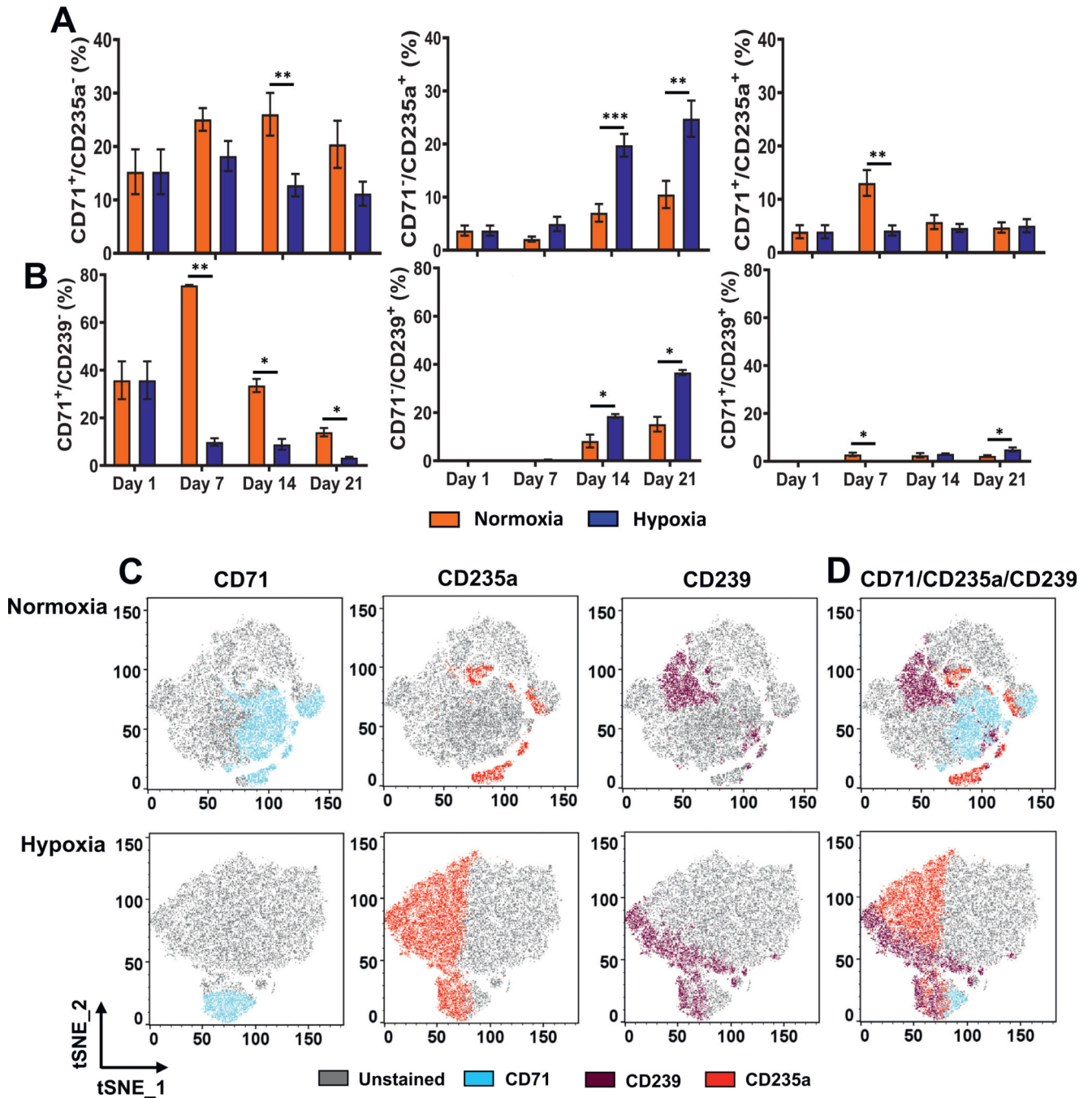
Figure 5.
Hypoxia enhances expression of erythroid markers. **(A)** Longitudinal analysis of CD71 relative to the erythroid marker CD235a in cultures incubated in normoxia or hypoxia. Percentages of $CD71^+/CD235a^-$, $CD71^-/CD235a^+$, and $CD71^+/CD235a^+$ in the $CD34^-$/Live population are illustrated. **(B)** Longitudinal analysis of CD71 relative to the erythroid marker CD239 in cultures incubated in normoxia or hypoxia. Percentages of $CD71^+/CD239^-$, $CD71^-/CD239^+$, and $CD71^+/CD239^+$ cells in the $CD34^-$/Live population are illustrated. Data are represented as the mean with standard error ($n = 4$). Statistical analysis was

performed using the Mann-Whitney test, and p values 0.05 were considered significant. **(C)** tSNE plots revealing distribution of CD71^{+}, CD235a^{+}, and CD239^{+} cells on day 21 in normoxia or hypoxia. **(D)** tSNE plots of overlay of CD71^{+}, CD235a^{+}, and CD239^{+} cells in normoxia or hypoxia on day 21. tSNE analysis was performed in FlowJo. $*p < 0.05$, $**p < 0.005$, $***p < 0.0005$.
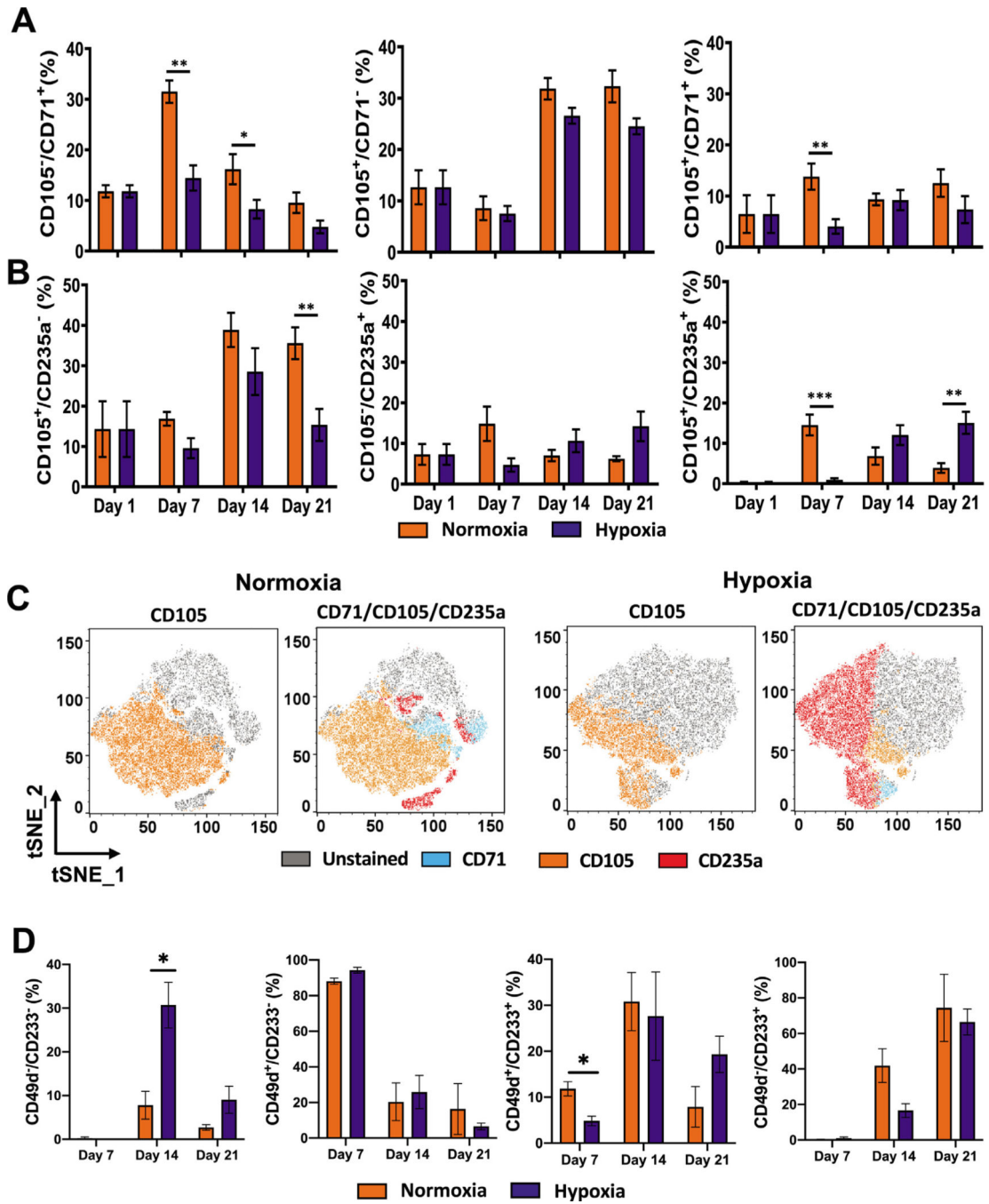
Figure 6.
Expression of CD105 is persistent in hypoxia. **(A)** Longitudinal analysis of CD71 and CD105 in cultures incubated in normoxia or hypoxia. Percentages of CD71⁺/CD105⁻, CD71⁻/CD105⁺, and CD71⁺/CD105⁺ in the CD34⁻/Live population are illustrated. **(B)** Longitudinal analysis of CD105 relative to the erythroid marker CD235a in cultures incubated in normoxia or hypoxia. Percentages of CD105⁺/CD235a⁻, CD105⁻/CD235a⁺, and CD105⁺/CD235s⁺ cells in the CD34⁻/Live population are illustrated. Data are represented as the mean with standard error ($n = 4$). Statistical significance was calculated

using the Mann-Whitney test, and p values 0.05 were considered significant. **(C)** tSNE plots revealing the distribution of CD105$^+$ cells and overlay of CD71$^+$, CD105$^+$, and CD235a$^+$ cells on day 21 in normoxia or hypoxia. tSNE analysis was performed in FlowJo. **(D)** Longitudinal analysis of the CD49d and CD233 in cultures incubated in normoxia or hypoxia. Percentages of CD49d$^-$/CD233$^-$, CD49d$^+$/CD233$^-$, CD49d$^+$/CD233$^+$, and CD49d$^+$/CD233$^-$ cells in the CD235a$^+$ population are illustrated. $*p < 0.05$, $**p < 0.005$, $***p < 0.0005$.
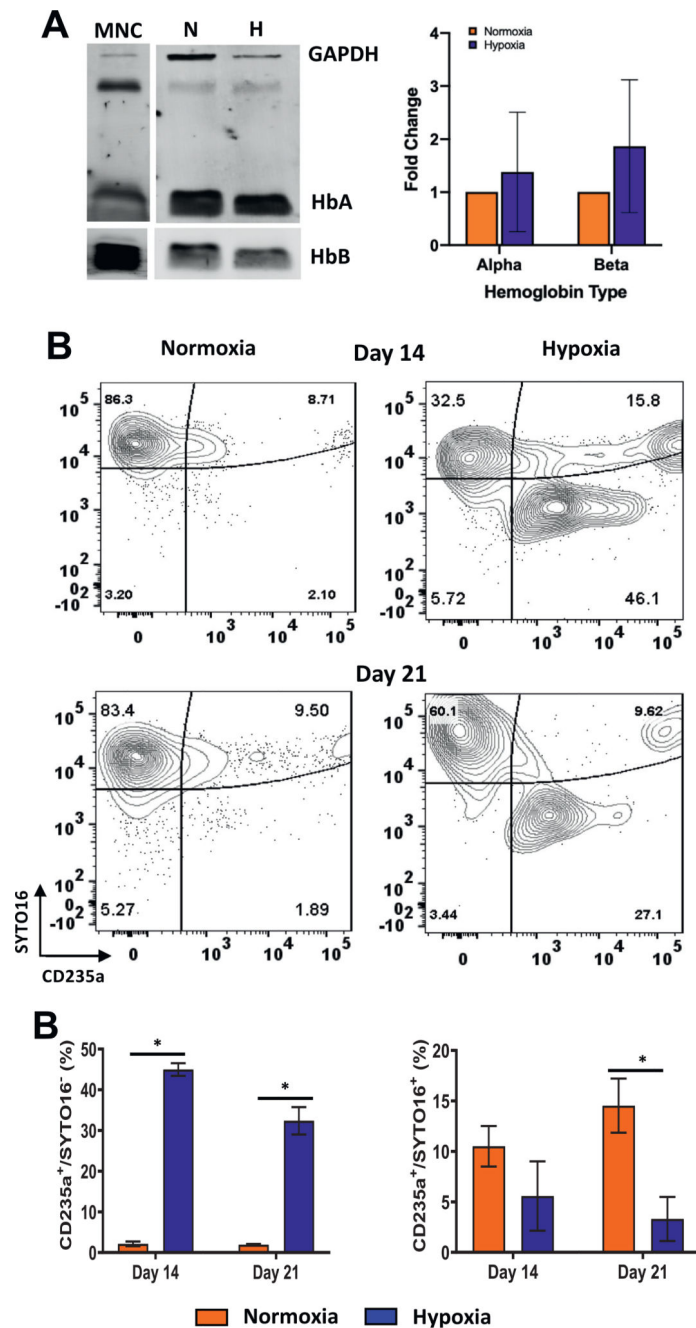
Figure 7.
Hypoxia promotes enuclation of erythroid cells. **(A)** Immunoblotting of α- and β-hemoglobin expression in CD34^{+} cell cultures incubated in normoxia or hypoxia and in cord blood-derived mononuclear cells (MNCs). Average protein expression (§SE, $n = 3$) normalized to GAPDH is illustrated. **(B)** Enuclation was determined by SYTO16 staining. Contour plots for CD235a^{+} and SYTO16^{+} cells in cultures incubated in hypoxia or normoxia. **(C)** Percentages of enuclated (CD235a^{+}/SYTO16^{−}) and nucleated (CD235a^{+}/SYTO16^{+}) erythroid cells in the CD34^{−}/Live population on days 14 and 21 are represented

as the mean with standard error ($n = 4$). Statistical analysis was performed using the Mann-Whitney test, and p values 0.05 were considered significant. *$p < 0.05$, **$p < 0.005$, ***$p < 0.0005$.